16TH EUROPEAN CONFERENCE ON EARTHQUAKE ENGINEERING THESSALONIKI 18 - 21 JUNE 2018

# 3D PHYSICS-BASED NUMERICAL MODELING AS A TOOL FOR SEISMIC RISK ASSESSMENT OF URBAN INFRASTRUCTURAL SYSTEMS: THE CASE OF THESSALONIKI, GREECE

Chiara SMERZINI[1], Francesco CAVALIERI[2], Sotiris ARGYROUDIS[3], Kyriazis PITILAKIS[4]

## ABSTRACT

The aim of this paper is to develop a seismic risk assessment study of urban infrastructural systems relying on state-of-the-art tools for the prediction of earthquake ground motion as well as the assessment of vulnerability. The proposed approach makes use, on one hand, of 3D physics-based numerical simulations of source-to-site wave propagation problems to provide an accurate description of spatial variability of ground shaking and, on the other hand, of systemic approaches for the evaluation of the vulnerability of complex, interconnected urban systems. The city of Thessaloniki, in Northern Greece, is taken as case study and the physical damage and loss of performance for the main water supply system are estimated based on connectivity based performance indicators. A couple of rupture scenarios with magnitude $M_W$ equal to 6.5 and 7.0, breaking two major hazardous faults around the city are used. The results indicated that 3D simulations can efficiently and accurately account for near-source conditions, geological and site conditions at local scale as well as for spatial and cross-correlation of ground motion. The risk estimates are compared with the ones obtained using a standard approach based on Ground Motion Prediction Equations (GMPEs), accounting for the spatial variability of ground motion. It was concluded that the GMPEs based approach can be used for a preliminary and faster seismic loss estimation. However, the results shed light on the main advantages of a full 3D numerical modeling for seismic risk assessment in large urban environments and spatially distributed systems. A major advantage is the more accurate estimation of spatial correlation of ground motion, which is location- and earthquake- specific.

*Keywords: seismic risk; 3D physics-based numerical modeling; systemic vulnerability; water supply system*

## 1. INTRODUCTION

Seismic risk studies are crucial to assess the socio-economic impact of an earthquake on a densely populated area, to plan effective actions for risk mitigation and emergency response. Key tools for such studies are, on one hand, a proper characterization of earthquake ground motion and of its spatial variability (hazard) and, on the other hand, reliable vulnerability models to establish a relationship between the hazard and the expected damage. The goal of this work is to present a novel approach for seismic risk assessment studies at urban scale using state-of-the-art tools both for the prediction of earthquake ground motion and for the assessment of seismic vulnerability of complex, urban, interconnected systems.

An improved assessment of seismic hazard was achieved using 3D physics-based numerical simulations of ground shaking, reproducing the physics of the whole seismic wave propagation problem, from the fault rupture up to the site of interest, as opposed to conventional empirical methods relying on Ground Motion Prediction Equations (GMPEs). 3D numerical simulations are suitable to

[1] Department of Civil and Environmental Engineering, Politecnico di Milano, Italy, chiara.smerzini@polimi.it
[2] Department of Structural Geotechnical Engineering, Sapienza University, Rome, Italy, francesco.cavalieri@uniroma1.it
[3] Department of Civil Engineering, Aristotle University of Thessaloniki, Greece, sarg@civil.auth.gr
[4] Department of Civil Engineering, Aristotle University of Thessaloniki, Greece, kpitilak@civil.auth.gr

overcome some shortcomings of the GMPEs, which: (i) are poorly constrained for large magnitude events and in near-source conditions that are of concern for the damage of structures; (ii) cannot account for the geological peculiarities of the area under study and the complex site conditions at local scale; (iii) cannot describe the spatial correlation and cross-correlation structure of ground motion. Referring to point (iii), it is recognized that risk and loss assessment of large urban areas with spatially distributed building portfolios and multiple interconnected infrastructural systems require an accurate description of spatial variability of ground motion intensity at regional scale as well as of cross-correlation of ground motion across different intensity measures, such as response spectral ordinates across different periods (Park et al. 2007; Weatherill et al. 2015; Baker and Jayaram 2008).
As regards damage assessment, state-of-the-art vulnerability models for interconnected infrastructural systems, as developed in SYNER-G (2012) project, were adopted. In particular, SYNER-G developed an innovative methodological framework for the assessment of physical as well as socio-economic seismic vulnerability at the urban/regional level. The built environment was modeled according to a detailed taxonomy into its component systems as close as possible to the European distinctive features of the construction practice, grouped into buildings, transportation and utility networks, and critical facilities. The framework encompasses all aspects in the chain, from regional hazard to fragility assessment of components to the socioeconomic impacts of an earthquake, accounting for relevant uncertainties within an efficient quantitative simulation scheme, and modeling interactions between the multiple component systems in the taxonomy. Fragility curves based on SYNER-G taxonomy were selected, developed and proposed for all elements at risk including damage scales, intensity measures and performance indicators (Pitilakis et al. 2014).
The proposed approach was applied to the city of Thessaloniki, where an abundance of data is available, to estimate the physical damage and loss of performance for the water supply system. Seismic risk was evaluated for a set of physics-based ground shaking scenarios generated through a large-scale spectral element model including the extended seismic source, the propagation from the source to the site as well as the 3D basin. Numerical simulations were carried out by the high-performance code SPEED (http://speed.mox.polimi.it/) described in Mazzieri et al. (2013). For these ground shaking scenarios, risk of the main water supply system of Thessaloniki was expressed in terms of probability of exceedance of service loss levels, measured by connectivity-based performance indicators. The variability of the expected losses within the urban area was also explored considering a set of different fault rupture scenarios. As an important outcome of this work, the SPEED-based damage and loss of performance estimates were compared with the ones obtained using a standard approach based on GMPEs, but accounting for the spatial variability of ground motion.

## 2. SEISMIC HAZARD: 3D PHYSICS-BASED NUMERICAL SIMULATIONS

3D numerical simulations of seismic wave propagation were performed using the Discontinuous Galerkin Spectral Elements Method (DGSEM) implemented in the open-source computer package called SPEED - SPectral Element in Elastodynamics with Discontinuous Galerkin (http://speed.mox.polimi.it/). SPEED can handle the simulation of large-scale seismic wave propagation problems including the coupled effect of a seismic fault rupture, the propagation path through Earth's layers and localized geological irregularities, such as alluvial valleys (Mazzieri et al, 2013). Based on a discontinuous version of the classical spectral element (SE) method, SPEED is naturally oriented to solve multi-scale numerical problems, allowing one to use non-conforming meshes (*h*-adaptivity) and different polynomial approximation degrees (*N*-adaptivity) in the numerical model. The code was optimized to run on multi-core computers and large clusters (e.g., Marconi at CINECA), taking advantage of the hybrid MPI-OpenMP parallel programming. Referring to earthquake engineering applications, the main features of the code include: i) different seismic excitation modes, from plane wave propagation to extended kinematic fault source models (as adopted in this work); ii) linear and non-linear visco-elastic soil materials; iii) different anelastic attenuation models with frequency proportional quality factor or frequency constant quality factor.

### *2.1 3D computational model*

Referring to Smerzini et al. (2017) for further details, a large-scale 3D spectral element model was

constructed, including the following features (see Figure 1):

- ground topography;
- kinematic source model of two major seismogenic faults posing a hazard to the city of Thessaloniki, namely, the Gerakarou fault (i.e., the source responsible of the $M_W$6.5 1978 Volvi earthquake) and the Anthemountas fault system;
- horizontally layered crustal model for deep rock materials;
- 3D subsoil model of the Thessaloniki urban area with homogeneous velocity profiles for Eurocode 8 – EC8 (CEN, 2004) sites B and C, calibrated on the basis of detailed microzonation geotechnical studies (Anastasiadis et al. 2001) and geophysical analyses (Apostolidis et al. 2004);
- non-linear visco-elastic soil behavior for top 100 m sediments (see Stupazzini et al. 2009 for the implementation details).

Note that the mesh extends over a volume of about 82 km x 64 km x 31 km and was discretized using an unstructured hexahedral conforming mesh with a total number of degrees of freedom of approximately 60 million. The maximum frequency of the numerical model is about 1.5 Hz.

### *2.2 Earthquake scenarios*

In this study two earthquake scenarios were considered: the historical 1978 June 20$^{th}$ Volvi earthquake, $M_W$6.5, rupturing the Gerakarou fault located northeast of Thessaloniki, and a hypothetical earthquake scenario with $M_W$7.0, occurring along the Anthemountas fault system, south of the city. Both faults are of normal type and a $k^{-2}$ slip distribution (Herrero and Bernard, 1994) was adopted to describe fault rupture (see superimposed maps in Figure 1).

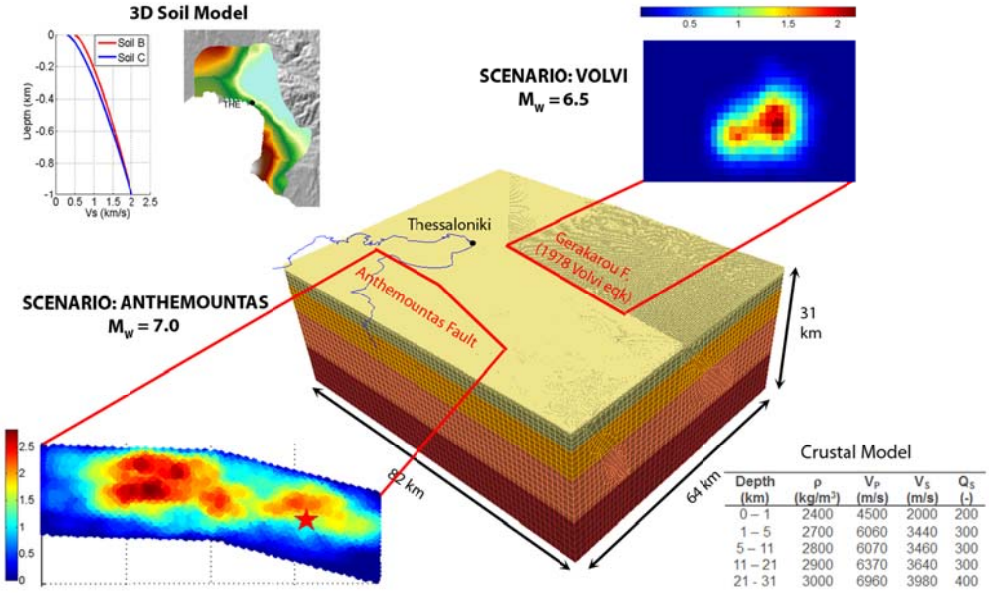


Figure 1. 3D numerical model adopted to generate the ground shaking scenarios: Volvi, $M_W$6.5 (1978 June 20$^{th}$ earthquake); Anthemountas, $M_W$7.0.

### *2.3 Main results*

As shown in the following sections, assessment of damage to the water supply system needs the Peak Ground Velocity (PGV) and the permanent ground deformation due to liquefaction. The latter, referred to in the following as PGD, is computed as a function of the Peak Ground Acceleration (PGA). To obtain accurate predictions of short period intensity measures, such as PGA, broadband ground shaking scenarios have to be produced starting from the 3D numerical simulations, which are reliable only in the low frequency range, specifically up to 1.5 Hz.

For this purpose, a novel approach based on Artificial Neural Network (ANN) was adopted here to generate broadband ground motions, as described in Paolucci et al. (2017). We limit herein to recall that, for any location, the low period range of the response spectrum is predicted by an ANN trained on a database of strong motion recordings of engineering significance (i.e. $M_W$=5-7+, epicentral distance < 35 km), which takes as input the long period response spectral ordinates from SPEED. The main advantage of such an approach, especially in the perspective of its use in seismic risk assessment studies, is that spatial correlation of ground motion is realistically reproduced.
Figure 2 shows a selection of results from SPEED in terms of spatial distribution of PGV, computed as geometric mean of horizontal components, for both scenarios (left: Volvi; right: Anthemountas). It is apparent the strong correlation of the map of PGV with the focal mechanism of the source model and directivity/directionality effects from the extended fault and with the 3D soil structure beneath the city and the Anthemountas basin. Note that risk analyses shown in Section 4 will be limited to the urban area of Thessaloniki, highlighted with black contour in Figure 2.

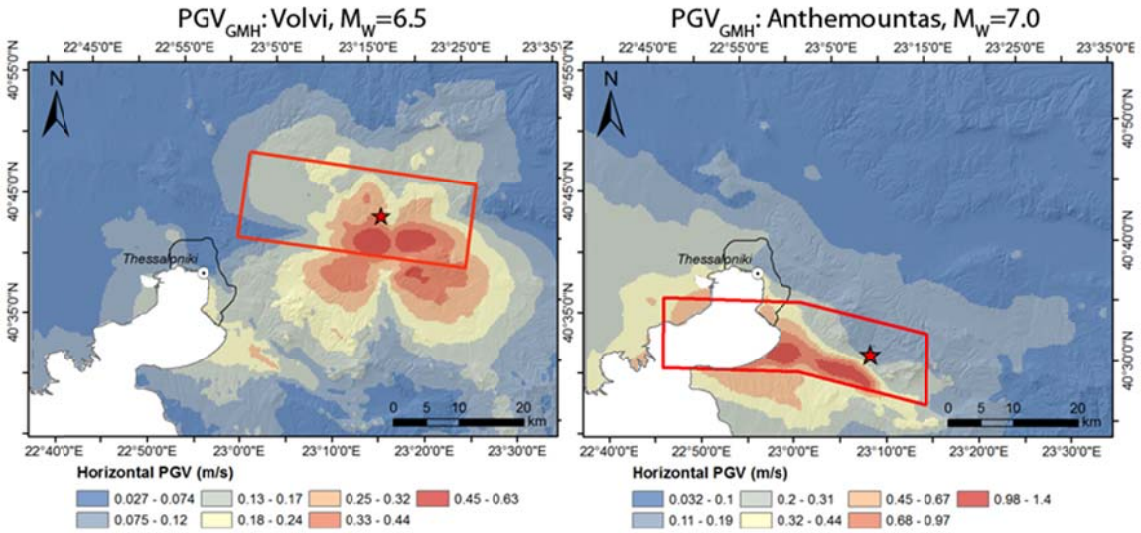


Figure 2. Spatial distribution of horizontal PGV (geometric mean) from 3D physics-based numerical simulations (SPEED) for both Volvi (left) and Anthemountas (right) scenarios.

## 3. SYSTEMIC SEISMIC VULNERABILITY: OOFIMS MODEL

A software platform for quantitative probabilistic seismic risk analysis, namely Object-Oriented Framework for Infrastructure Modeling and Simulation (OOFIMS), has been recently developed (Franchin and Cavalieri n.d., 2013) within SYNER-G (2012), as a computational tool to assess the vulnerability and risk to earthquakes of an urban area including buildings, lifelines and critical facilities. The tool, coded in MATLAB® (The MathWorks 2011) language according to the object-oriented paradigm (OOP), allows to model and analyze the performance of interconnected/interdependent infrastructure systems and sets of buildings, at the urban/regional scale, in ordinary or "disturbed" conditions (e.g., due to the impact of a natural or man-made hazard). In abstract terms, within the OOP, a problem is described as a set of objects that interact with each other. Objects are instances (concrete realizations) of classes (abstract models or templates for all objects with the same set of properties and methods). Each class is defined by its attributes (properties that all objects from the class possess) and methods (actions that objects from the class can perform). The object model developed within SYNER-G and implemented in OOFIMS is described by means of *class diagrams*. As an example, Figure 3 shows the class diagram for the water supply system (WSS) and the electric power network (EPN) in OOFIMS. Both the WSS and EPN classes are composition of the corresponding node and edge classes. The latter, in general, are abstract classes, since there can be several types of edges and nodes within a network, differentiated in terms of properties and functions. For instance, for the water supply system, edges can either be pipes or tunnels, while nodes can be end-user demand nodes, water sources or pumping stations. The *Water source* class is an abstract one,

since there can be both variable head (like elevated tanks) and constant head (like large reservoirs) water sources. As far as the electric-power network is concerned, edges can be either overhead or buried lines, and there are three node types: end-user demand nodes (load buses), electric power sources (generators) and balance nodes (slack buses, one per network). Load buses can be either distribution (D) or transformation/distribution substations (TD). These nodes are assemblies of several microcomponents. The two networks are shown in the same figure to highlight the interdependence between them, represented by the (*association*) link between the pumping station class in the WSS and the distribution (or transformation/distribution) class in the EPN.

Uncertainty in OOFIMS is treated with a set of random variables that describe single random quantities or discretized random fields. Values of such random variables are sampled from their distributions in a Monte Carlo simulation. Concerning the hazard model, in each simulation run (one event or scenario), the source $S$ is sampled first, from a discrete distribution with probability mass proportional to $\lambda_0$, i.e., the mean annual rate of events on the sources. Given the source, magnitude $M$ is sampled from the Gutenberg-Richter recurrence law. The location $L$ is then sampled within source $S$ (with probability depending on the source model, uniform for area sources). Given $M$ and $L$, the inter- and intra-event (the latter spatially correlated) errors $\eta$ and $\varepsilon$ in a ground-motion prediction equation are sampled to obtain a chosen primary IM, for example PGA, on a square grid on rock. Such IM is then interpolated, from the closest four grid points, to the vulnerable components' sites. Conditional on the primary IM, all further IMs needed in fragility models can be sampled. Surface intensity values are then obtained with random amplification functions. Permanent ground deformation (PGD) due to geotechnical hazards is finally obtained with relevant models, such as the FEMA/HAZUS (2003) model where landslide and liquefaction probability is a function of surface PGA. Details can be found in Franchin and Cavalieri (2013). The goal of the present work, as already mentioned, is the comparison between the GMPE-based (i.e., OOFIMS-based) hazard model with the 3D physics-based numerical ground motion shaking scenarios (i.e., SPEED-based). Since the latter is specified in terms of a deterministic scenario event, with fixed magnitude and hypocenter, these quantities were fixed also in the GMPE-based simulations, so that scenario-based hazard scenarios will be considered herein. The GMPE by Akkar and Bommer (2010), recently developed for the European context, was used in this work. The model proposed by Jayaram and Baker (2009) was adopted for the spatial correlation of the intra-event error term. Specifically, an exponential model was adopted to describe the spatial correlation structure of the intra-event error term associated with the GMPEs. PGA was chosen to be the primary IM, that is, the only one that is sampled on a square grid using the spatial correlation model. Based on the studies performed by Esposito and Iervolino (2011; 2012) on the European strong motion database, in this model the maximum distance beyond which the motions are uncorrelated, termed *range*, was set to 13.5 km for PGA. The size of the square grid for prediction of the primary IM on rock was set to 0.5 km, which, compared to the adopted range values, allows a proper consideration of spatial correlation of intra-event residuals.

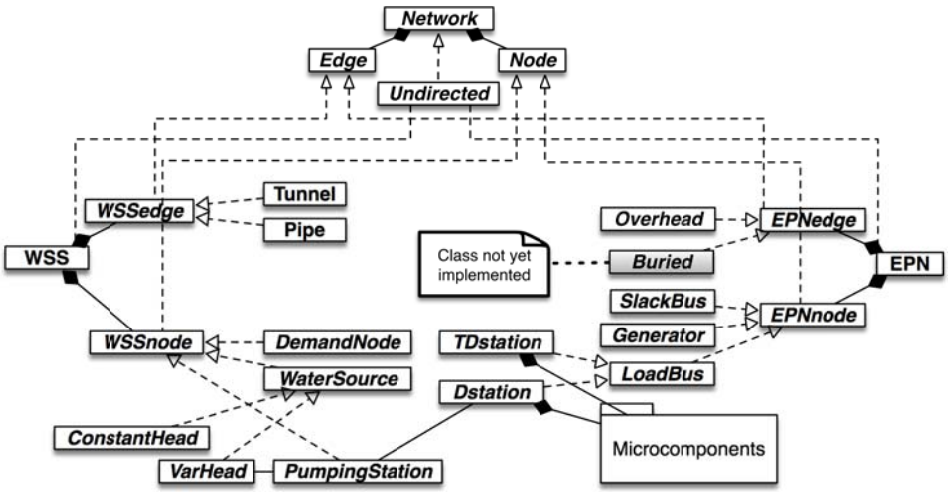


Figure 3. Class diagram for the WSS and EPN classes (Franchin 2014).

Once values for the appropriate IMs at the surface are known at each site, the physical damage state of each component is sampled. This is done differently for point-like and line-like components, with fragility curves used for the former, and Poisson rates as a function of the intensity for the latter. The Poisson rate $\lambda$ is usually employed to describe the rate of faults (leaks/breaks) per unit length, and is experimentally derived from repair rates obtained in post-earthquake damage surveys. In the WSS model within OOFIMS, only pipelines are considered as vulnerable to earthquakes and the fragility model is given in terms of two Poisson repair rates per kilometer, functions of peak ground velocity (PGV, in cm/s) and PGD (in m), respectively (ALA 2001):

$$\begin{aligned} \lambda_{\text{repair}}\left(\text{PGV}\right) &= K_1 \cdot 0.0024 \cdot \text{PGV} \\ \lambda_{\text{repair}}\left(\text{PGD}\right) &= K_2 \cdot 11.224 \cdot \text{PGD}^{0.319} \end{aligned} \tag{1}$$

where $K_1$ and $K_2$ are functions of the pipe material, soil, joint type and diameter and $\lambda_{\text{repair}}$ is returned in $\text{km}^{-1}$. The number of leaks/breaks, $N_L$ for the generic pipe is randomly generated using the highest repair rate as the mean of the Poisson distribution. If $N_L > 0$, a number $N_L$ of standard uniform numbers is sampled and compared with the rupture probability (a function of $\lambda$). If at least one is lower than the rupture probability, the pipe is broken and removed from the network. Since in this study a connectivity-based WSS analysis was carried out, the water outflow from leaks/breaks was not retrieved. In OOFIMS it is possible to carry out a capacitive analysis on the WSS, with computation of flow in pipes and water head at demand nodes.

## 4. RISK ASSESSMENTS FOR THE WATER SYSTEM OF THESSALONIKI

### *4.1 Water Supply System of Thessaloniki*

The water supply system of the municipality of Thessaloniki includes 20 tanks with total capacity of 91,900 $\text{m}^3$. There is also a sedimentation tank of 8,000 $\text{m}^3$ capacity and a fire-fighting tank with total capacity of 2,100 $\text{m}^3$. The main transmission system has a total length of about 71 km, while the distribution network has a 1,284.1 km approximate length and a supply capacity ranging between 240,000 - 280,000 $\text{m}^3$/day. The supplied customers are approximately 420,000 and the total supplied population is about one million. The supplied area is approximately 55 $\text{km}^2$; the elevation ranges from 0 to 380 m, and the water pressure between 2 and 5 bars.

For the needs of the present application and due to the complexity and oldness of the system, a simplified, yet realistic, model for Thessaloniki's main WSS was used (Argyroudis et al. 2014). This network is comprised of 477 nodes and 601 edges (pipes) with total length of about 280 km. The nodes were subdivided into 445 demand nodes, 21 elevated tanks served by pumping stations and 11 constant-head tanks (see Figure 4). Tanks were considered as water sources for the system. Pipelines have 24 different diameter values, ranging between 500-3,000 mm and their construction materials include asbestos cement, cast iron, PVC and welded steel.

The soil formations of the study area were classified according to the EC8 classification scheme (i.e., A, B, C soil classes). The liquefaction susceptibility was defined following the method adopted in HAZUS (FEMA 2003) on the basis of deposit type, age and general distribution of cohesionless loose sediments.

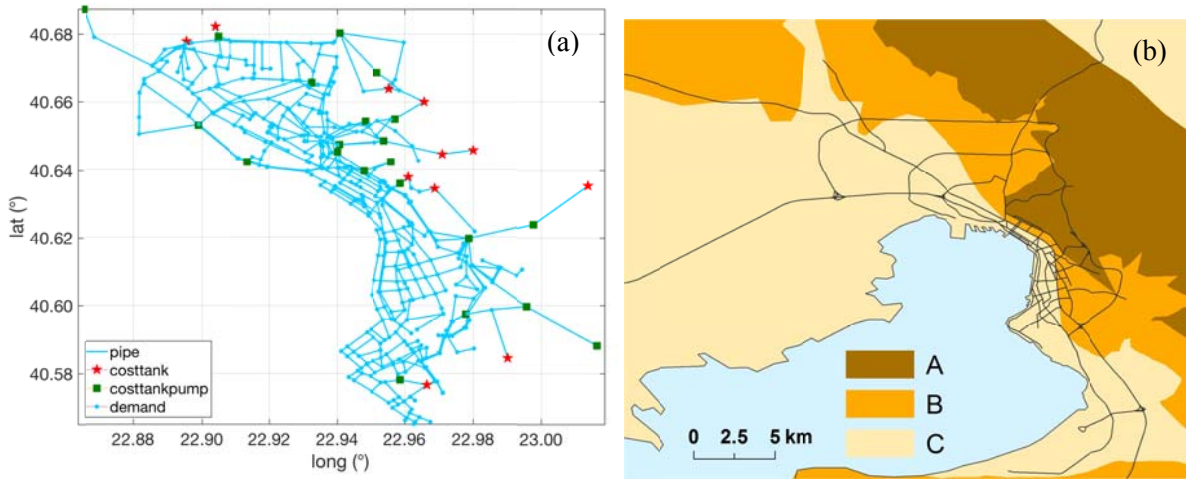


Figure 4. (a) The Thessaloniki water supply system used as case study; elements can be pipes, demand nodes, tanks and pumping stations, (b) Soil classification in the study area according to EC8.

### *4.2 Performance metrics*

In order to estimate the impact on the WSS performance due to the considered hazard models (GMPE-based and SPEED-based) and to carry out a comparison between them, four connectivity-based performance metrics were used, two of which are global, i.e. referred to the whole system, while the others are local, i.e. referred to the single pipes. The metrics are defined as follows:

• *Connectivity Loss, CL* (global, Poljanšek et al. 2012). CL, ranging between 0 and 1, is computed as in Eq. (2), counting the number of source nodes connected to the *i*-th demand node in the original (undamaged) network, $N^i_{\text{source,orig}}$, and in the damaged network, $N^i_{\text{source,dam}}$, and then averaging over all demand nodes (<···> denotes average).

$$\text{CL} = 1 - \left\langle \frac{N^i_{\text{source,dam}}}{N^i_{\text{source,orig}}} \right\rangle_i \tag{2}$$

• *Connectivity-based System Serviceability Index, $SSI_{conn}$* (global, Cavalieri et al. 2014). This metric was adapted from a flow-based one, SSI (Wang and O'Rourke 2008), which is defined as the ratio of the sum, over the $n$ demand nodes, of the delivered water flows after an earthquake, $Q_{i,s}$, to the sum of the water demands, $Q_{i,0}$ (delivered before the earthquake). In the current connectivity-based methodology, $\text{SSI}_{\text{conn}}$, ranging between 0 and 1, is defined as in Eq. (3), where $Q_{i,0}$ is the water demand at node $i$ and the weight $w_i$ is set to 1 if the $i$-th demand node is connected to at least one source node, and to 0 otherwise. Such weight is used to reduce the total delivered water flow in case of disconnection of demand nodes from sources.

$$\text{SSI}_{\text{conn}} = \frac{\sum_{i=1}^{n} Q_{i,0} \cdot w_i}{\sum_{i=1}^{n} Q_{i,0}} \tag{3}$$

• *Upgrade Benefit Index, UBI* (local, Wang et al. 2010). This metric was first defined for application with SSI, in a flow-based analysis. In this work, UBI was computed with $\text{SSI}_{\text{conn}}$, but the original expression was adopted. UBI measures the impact of the upgrade of an individual pipe on the overall system serviceability, and is used to identify critical pipes that significantly affect the system seismic performance. It is defined as in Eq. (4), where $m_1$ is the total number of simulation runs and $m_2$ is the number of samples where the $i$-th pipe is intact. By "upgrade" it is meant that the probability of pipe breakage given an earthquake is significantly smaller than its value before upgrade. $\text{UBI}_i$ is the percent increase of $\text{SSI}_{\text{conn}}$ given that the $i$-th pipe is upgraded.

$$\mathrm{UBI}_i = \frac{\mathrm{E}\left[\mathrm{SSI}_{\mathrm{conn}} \mid \text{pipe } i \text{ upgrade}\right] - \mathrm{E}\left[\mathrm{SSI}_{\mathrm{conn}}\right]}{1 - \mathrm{E}\left[\mathrm{SSI}_{\mathrm{conn}}\right]} \cong \frac{\frac{1}{m_2}\sum_{j=1}^{m_2}\mathrm{SSI}_{\mathrm{conn},j} - \frac{1}{m_1}\sum_{k=1}^{m_1}\mathrm{SSI}_{\mathrm{conn},k}}{1 - \frac{1}{m_1}\sum_{k=1}^{m_1}\mathrm{SSI}_{\mathrm{conn},k}} \tag{4}$$

• Damage Consequence Index, DCI (local, Wang et al. 2010). Like UBI, this metric was first defined for application with SSI, and here it has been computed with $\mathrm{SSI}_{\mathrm{conn}}$, while keeping the original expression. DCI is a measure of the impact of a pipe breakage on the overall system serviceability. It is defined as in Eq. (5), where $m_1$ is the total number of simulation runs and $m_3$ is the number of samples where the $i$-th pipe is broken. $\mathrm{DCI}_i$ is the percent reduction of $\mathrm{SSI}_{\mathrm{conn}}$ given that the $i$-th pipe is broken.

$$\mathrm{DCI}_i = \frac{\mathrm{E}\left[\mathrm{SSI}_{\mathrm{conn}}\right] - \mathrm{E}\left[\mathrm{SSI}_{\mathrm{conn}} \mid \text{pipe } i \text{ broken}\right]}{1 - \mathrm{E}\left[\mathrm{SSI}_{\mathrm{conn}}\right]} \cong \frac{\frac{1}{m_1}\sum_{k=1}^{m_1}\mathrm{SSI}_{\mathrm{conn},k} - \frac{1}{m_3}\sum_{j=1}^{m_3}\mathrm{SSI}_{\mathrm{conn},j}}{1 - \frac{1}{m_1}\sum_{k=1}^{m_1}\mathrm{SSI}_{\mathrm{conn},k}} \tag{5}$$

### *4.3 Results and discussion*

Four Monte Carlo simulations were carried out, to allow the combinations of the two considered ground motion scenarios (Volvi and Anthemountas, see Section 2.2) and the two different hazard models (SPEED-based and GMPE-based). To investigate the sensitivity of results to the spatial correlation of IMs, two more simulations were added, one per scenario, employing the GMPE-based model in which the spatial correlation of primary IM values was disregarded. In the GMPE-based case, the IMs of interest (i.e., PGV and PGD) were computed by the procedure outlined in Section 3 (and implemented in OOFIMS). On the other hand, when defining the hazard by means of physics-based simulations, PGA and PGV were provided by the offline SPEED broadband computations (see Section 2.3). Note that liquefaction-induced PGD is not provided as an output by SPEED and hence it was retrieved by the OOFIMS geotechnical hazard module in which it is derived based on the PGA estimates from SPEED using empirical relationships. All simulations consisted of just 1,000 runs each, given the reduced uncertainty in the hazard models: in fact, the IMs from SPEED are constant in all simulation runs, while in the GMPE-based approach magnitude and hypocenter were fixed, so that only the epistemic uncertainty in the motion attenuation, amplification and geotechnical hazard was considered. The epistemic uncertainty associated with vulnerability assessment is also present (see Section 3), and is the same for all the simulations.

Figure 5 shows the comparison between the Cumulative Distribution Functions (CDFs) of CL and $\mathrm{SSI}_{\mathrm{conn}}$, from the SPEED-based simulation, for both events. It is noted that, although in the Volvi scenario more significant directivity effects were found to occur, the Anthemountas scenario results to be the most damaging, in terms of both connectivity loss and serviceability, owing mainly to the higher magnitude and smaller source-to-site distance.

Results were also retrieved at the component (i.e., pipe) level, using the two local performance metrics adopted, namely UBI and DCI. Due to page limit, only the results in terms of UBI are reported here, given the more relevance of this index compared to DCI: in fact, UBI is the primary index in seismic mitigation, and critical links are pipes with relatively large UBI values (Wang et al. 2010). Figure 6 shows UBI maps, from the SPEED-based simulation, for both events. UBI values exist at pipe centroid sites. Instead of interpolating and extrapolating values, both figures are presented as Voronoi diagrams, in which each pipe is assigned a uniformly colored Voronoi cell, collecting all points for which the centroid of that pipe is the closest point. In this representation, UBI values for a pipe are extended to its entire Voronoi cell: moreover, adjacent cells with the same color are merged. The maps indicate the presence of critical links, meaning pipes that result to be damaged in the simulation and whose upgrade will benefit more the system serviceability. Looking at the maps, it appears clear that the Anthemountas scenario causes more pipes to be damaged and thus attain a UBI value larger than zero (see Figure 6(b)). It is also noted that most damage is expected towards south-east of the city,

which is closer to Anthemountas fault. Therefore, these results confirm the conclusions drawn for the system-level metrics, that is, the most severe impact of the Anthemountas scenario, compared to the Volvi event. The different orders of magnitude attained by UBI in the two maps are also due to the expected value of $SSI_{conn}$, which is different for the two scenarios (see Figure 5(b)).

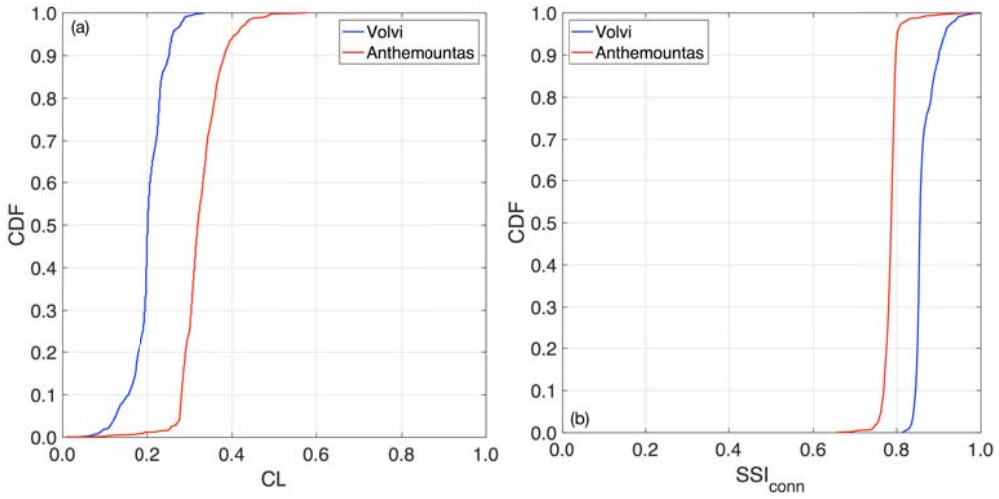


Figure 5. CDFs of (a) CL and (b) $SSI_{conn}$ provided by the SPEED-based simulation, for both scenarios.

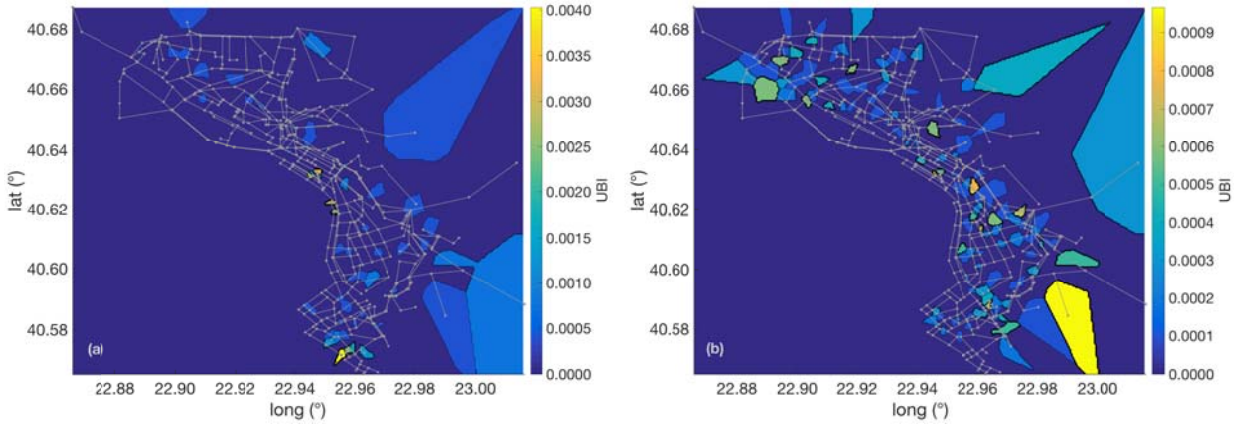


Figure 6. Voronoi diagrams of UBI provided by the SPEED-based simulation, for the (a) Volvi and (b) Anthemountas scenarios.

In order to investigate the difference in impact of the two hazard models on the employed system-level metrics, the CDFs of CL and $SSI_{conn}$ provided by the SPEED-based and GMPE-based simulations were compared, with reference to the most critical scenario, i.e. the Anthemountas earthquake. Results are displayed in Figure 7, where the effect of considering a spatial correlation model for intra-event residuals of the GMPE is also highlighted. It can be noted in the figure a substantial divergence between the SPEED-based and GMPE-based curves: in particular, the SPEED-based simulation always yield more damaging results, with higher values of connectivity loss and lower values of serviceability. Such differences are mainly related to the higher IMs predicted by the physics-based approach for the particular earthquake scenario, because of the combination of near-source effects (consider that the southern sector of the city lies on the surface projection of the fault, see Figure 2) with 3D complex site effects, which cannot be reproduced by median empirical estimates. It should be recalled that, while GMPEs produce median estimates, based on empirical regressions made on different earthquakes and site conditions of the same type, the physics-based approach produces a single earthquake realization, which may be more or less "favorable" in terms of seismic risk in the city, depending on details of rupture process (slip distribution, source-to-site azimuth) and specificity of local geologic conditions. It has to be remarked, however, that the results are not completely

incomparable, and this confirms that a GMPE/spatial correlation/amplification model can still be used for a quick and preliminary estimate of seismic loss. On the other hand, the consideration of spatial correlation in the GMPE-based simulation does not affect significantly the results in this particular application, leading to a slightly worse network performance, due to more severe damage, in terms of both connectivity loss and serviceability. The sensitivity of the results to the spatial correlation model adopted is object of future work.

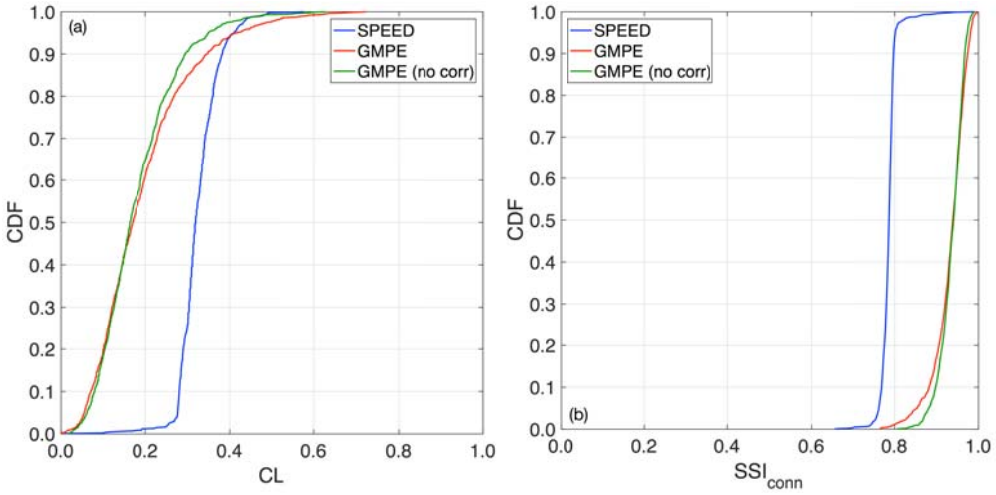


Figure 7. Anthemountas scenario. CDFs of (a) CL and (b) $SSI_{conn}$ provided by the SPEED-based and GMPE-based simulations, the latter with and without spatial correlation.

## 5. CONCLUSIONS

This paper has presented a seismic risk assessment study at urban scale combining latest-generation tools for both prediction of earthquake ground motion and assessment of systemic vulnerability of interconnected urban systems. To achieve this aim, the numerical codes developed independently by the research teams at Politecnico di Milano and at the University of Rome La Sapienza, namely a spectral element code for 3D physics-based numerical modeling of ground shaking (SPEED) and an object-oriented tool for infrastructure modeling and simulation (OOFIMS), have been used and interconnected. To test the feasibility of the proposed approach, the physical damage and loss of performance for the water supply system of the city of Thessaloniki has been estimated considering a couple of 3D physics-based ground shaking scenarios, with $M_W$ equal to 6.5 and 7, originating from two of the most hazardous active faults around the city (Volvi and Anthemountas).

Although this study addresses only two seismic rupture scenarios, neglecting the aleatory uncertainty associated with the fault rupture model, it has been demonstrated that 3D physics-based numerical simulations of source-to-site wave propagation have become mature enough to be incorporated in seismic risk analyses at urban scale. At the level of a city, the impact of using physics-based simulations to describe the hazard is recognized mainly in its superiority to describe the spatial correlation of ground motion, accounting explicitly for the specificity of local geological conditions and source rupture features. To enhance this point, Figure 8 shows the comparison of the spatial correlation coefficient (assuming an exponential model) for PGV as adopted in OOFIMS (based on literature models calibrated on strong motion recordings) and derived from SPEED results for both scenarios. It is apparent that spatial correlation structure is location- and earthquake-specific (as also confirmed by other studies, see Infantino et al. 2018) and this may play a major role in seismic risk estimates. Future work will aim at extending the analysis and comparison with the GMPE-based approach to a wider set of rupture scenarios.

However, the findings included in this contribution suggest that a GMPE/spatial correlation/amplification model can still be used for a quick and more affordable estimate of IMs and future work will aim at extending the comparison between the two approaches. Within the latter approach, it would be possible to reduce the epistemic uncertainty by considering more models (source, GMPEs, spatial correlation, amplification) and then weighting them, for instance within a

logic tree approach. Future work will aim to properly treat such epistemic uncertainty and to repeat the comparison for a capacitive analysis, involving the computation of the operational state (flow in pipes and water head at demand nodes) including network connectivity.

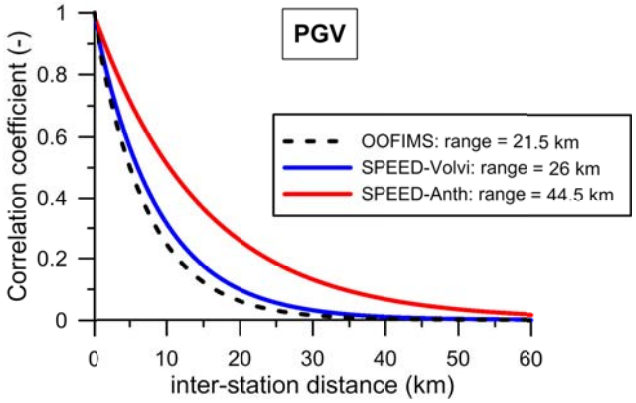


Figure 8. Comparison of spatial correlation coefficient (exponential model) for *PGV* as adopted in OOFIMS and derived from SPEED simulations, for both Volvi and Anthemountas scenarios. Range values are also shown.

## 6. ACKNOWLEDGMENTS

This research has been partially funded by the European Commission within the STREST Project, EU FP7/2007-2013, grant agreement no. 603389. The collaboration of the AUTH Scientific Computing Center is greatly acknowledged.

## 7. REFERENCES

Akkar S, Bommer JJ (2010). Empirical equations for the prediction of PGA, PGV and spectral accelerations in Europe, the Mediterranean region and the Middle East, *Seismological Research Letters*, 81(2): 195–206.

ALA (American Lifelines Alliance) (2001). Seismic Fragility Formulations for Water Systems. Part 1 - Guideline. ASCE-FEMA, Reston, VA, 104 p.

Anastasiadis A, Raptakis D, Pitilakis K (2001). Thessaloniki's detailed microzoning: subsurface structure as basis for site response analysis, *Pure appl. Geophys.*, 158: 2597-2633.

Apostolidis P, Raptakis D, Roumelioti Z and Pitilakis K (2004). Determination of S-wave velocity structure using microtremors and SPAC method applied in Thessaloniki (Greece), *Soil Dyn. Earthq. Eng.*, 24: 49-67.

Argyroudis S, Selva J, Kakderi K, Pitilakis K (2014). Application to the city of Thessaloniki. In: Pitilakis K et al. (eds) SYNER-G: Systemic seismic vulnerability and risk assessment of complex urban, utility, lifeline systems and critical facilities. Methodology and applications. *Geotechnical, Geological & Earthquake Eng.* 31, Springer.

Baker JW, Jayaram N (2008). Correlation of spectral acceleration values from NGA ground motion models. *Earthq Spectra*, 24(1): 299–317.

Cavalieri F, Franchin P, Buriticá Cortés JAM, Tesfamariam S (2014). Models for seismic vulnerability analysis of power networks: comparative assessment, *Computer-Aided Civil and Infrastructure Engineering*, 29(8): 590-607.

CEN, European Committee for Standardization (2004). Eurocode 8: Design Provisions for Earthquake Resistance of Structures, Part 1.1: General Rules, Seismic Actions and Rules for Buildings.

Esposito S, Iervolino I (2011). PGA and PGV spatial correlation models based on European multievent datasets, *Bulletin of the Seismological Society of America*, 101(5): 2532–41.

FEMA (2003). HAZUS-MH Technical Manual. Federal Emergency Management Agency, Washington DC, USA.

Franchin P, Cavalieri F (2013). Seismic vulnerability analysis of a complex interconnected civil infrastructure. In Tesfamariam S & Goda K (eds) Handbook of seismic risk analysis and management of civil infrastructure

systems, Woodhead Publishing Limited, Cambridge, UK, ISBN-13: 978 0 85709 268 7. DOI: 10.1533/9780857098986.4.465.

Franchin P (2014). A computational framework for systemic seismic risk analysis of civil infrastructural systems. In: Pitilakis K et al. (eds) SYNER-G: Systemic seismic vulnerability and risk assessment of complex urban, utility, lifeline systems and critical facilities. Methodology and applications. *Geotechnical, Geological & Earthquake Eng.* Vol. 31, Springer, Dordrecht. p. 23-56.

Herrero A, Bernard P (1994). A kinematic self-similar rupture process for earthquakes. *Bull Seismol Soc Am* 84(4): 1216-1228.

Infantino M, Paolucci R, Smerzini C, Stupazzini M (2018). Study on the spatial correlation of ground motion intensity by means of physics-based scenarios. Proceedings of the 16th European Conference on Earthquake Engineering, Thessaloniki, 18-21 June 2018 (*submitted*).

Jayaram, N, Baker JW (2009). Correlation model of spatially distributed ground motion intensities, *Earthq Eng Struct Dyn*, 38(15): 1687–708.

Mazzieri I, Stupazzini M, Guidotti R, Smerzini C (2013). SPEED: Spectral elements in elastodynamics with Discontinuous Galerkin: a non-conforming approach for 3D multi-scale problems. *Int J Numer Meth Eng*, 95 (12): 991–1010.

Franchin P, Cavalieri F n.d. OOFIMS Object-Oriented Framework for Infrastructure Modeling and Simulation. https://sites.google.com/a/uniroma1.it/oofims/. Accessed 1 Dec 2017.

Paolucci R, Gatti F, Infantino M et al (2017). Broad-band ground motions from 3D physics-based numerical simulations using artificial neural networks. *Bull Seismol Soc Am* (submitted for review).

Park J, Bazzurro P, Baker JW (2007). Modeling spatial correlation of ground motion intensity measures for regional seismic hazard and portfolio loss estimation. *In: Kanda J, Takada T, Furuta H (eds) Applications of statistics and probability in civil engineering.* Taylor & Francis, London.

Pitilakis K, Crowley H, Kaynia A. (Eds.) (2014). SYNER-G: Typology definition and fragility functions for physical elements at seismic risk, buildings, lifelines, transportation networks and critical facilities. *Geotechnical, Geological and Earthquake Engineering*, Vol. 27, Springer, Dordrecht.

Poljanšek K, Bono F, Gutiérrez E (2012). Seismic risk assessment of interdependent critical infrastructure systems: the case of European gas and electricity networks. *Earthq Eng Struct Dyn*, 41(1): 61-79.

Smerzini C, Pitilakis K, Hashemi K (2017). Evaluation of earthquake ground motion and site effects in the Thessaloniki urban area by 3D finite-fault numerical simulations. *Bull Earthquake Eng*, 15: 787–812.

Stupazzini M, Paolucci R, Igel H (2009). Near-fault earthquake ground-motion simulation in the Grenoble Valley by a high-performance spectral element code. *Bull Seismol Soc Am*, 99(1): 286-301.

SYNER-G (2012). Collaborative Research Project, funded by the European Union within Framework Programme 7 (2007–2013), under Grant Agreement no. 244061. www.vce.at/SYNER-G. Accessed 1 Dec 2017.

The MathWorks Inc. (2011). MATLAB® R2011b, Natick, MA.

Wang Y, Au SK, Fu Q (2010). Seismic risk assessment and mitigation of water supply systems. *Earthquake Spectra*, 26(1): 257-274.

Wang Y, O'Rourke TD (2008). Seismic performance evaluation of water supply systems. Technical Report MCEER-08-0015.

Weatherill GA, Silva V, Crowley H, Bazzurro P (2015). Exploring the impact of spatial correlations and uncertainties for portfolio analysis in probabilistic seismic loss estimation. *Bull Earthquake Eng*, 13: 957–981.